Published in final edited form as:

Sci Transl Med. 2013 August 28; 5(200): 200ra115. doi:10.1126/scitranslmed.3006373.

Molecular Mechanism for Age-Related Memory Loss: The Histone-Binding Protein RbAp48

Elias Pavlopoulos[1,2,3], **Sidonie Jones**[4,5,*], **Stylianos Kosmidis**[1,2,3,*], **Maggie Close**[1], **Carla Kim**[1], **Olga Kovalerchik**[1], **Scott A. Small**[4,5,†], and **Eric R. Kandel**[1,2,3,†]

[1]Department of Neuroscience, Columbia University, New York, NY 10032, USA

[2]Kavli Institute for Brain Science, Columbia University, New York, NY 10032, USA

[3]Howard Hughes Medical Institute, Columbia University, New York, NY 10032, USA

[4]Department of Neurology, Columbia University, New York, NY 10032, USA

[5]Taub Institute for Research on Alzheimer's Disease and the Aging Brain, Columbia University, New York, NY 10032, USA

Abstract

To distinguish age-related memory loss more explicitly from Alzheimer's disease (AD), we have explored its molecular underpinning in the dentate gyrus (DG), a subregion of the hippocampal formation thought to be targeted by aging. We carried out a gene expression study in human postmortem tissue harvested from both DG and entorhinal cortex (EC), a neighboring subregion unaffected by aging and known to be the site of onset of AD. Using expression in the EC for normalization, we identified 17 genes that manifested reliable age-related changes in the DG. The most significant change was an age-related decline in RbAp48, a histone-binding protein that modifies histone acetylation. To test whether the RbAp48 decline could be responsible for age-related memory loss, we turned to mice and found that, consistent with humans, RbAp48 was less abundant in the DG of old than in young mice. We next generated a transgenic mouse that expressed a dominant-negative inhibitor of RbAp48 in the adult forebrain. Inhibition of RbAp48 in young mice caused hippocampus-dependent memory deficits similar to those associated with aging, as measured by novel object recognition and Morris water maze tests. Functional magnetic resonance imaging studies showed that within the hippocampal formation, dysfunction was selectively observed in the DG, and this corresponded to a regionally selective decrease in histone

†Corresponding author. erk5@columbia.edu (E.R.K.); sas68@columbia.edu (S.A.S.).
*These authors contributed equally to this work.

SUPPLEMENTARY MATERIALS

www.sciencetranslationalmedicine.org/cgi/content/full/5/200/200ra115/DC1

Reference (*50*)

Author contributions: E.P. generated the RbAp48-DN mice, designed and contributed to all the mouse studies, analyzed the data, and wrote the manuscript. S.J. analyzed the microarray and fMRI data. S.K. analyzed RbAp48 protein level in young versus old wild-type mice and contributed to the HAT assays. C.K. examined histone acetylation. O.K. and M.C. performed behavioral studies. S.A.S. designed the human studies, analyzed the data, and wrote the manuscript. E.R.K. helped design the animal studies, analyzed the data, and wrote the manuscript. All authors discussed the results and commented on the manuscript.

Competing interests: The authors declare that they have no competing interests.

Data and materials availability: The microarray data are publicly available in the Gene Expression Omnibus database under accession number GSE46193.

acetylation. Up-regulation of RbAp48 in the DG of aged wild-type mice ameliorated age-related hippocampus-based memory loss and age-related abnormalities in histone acetylation. Together, these findings show that the DG is a hippocampal subregion targeted by aging, and identify molecular mechanisms of cognitive aging that could serve as valid targets for therapeutic intervention.

INTRODUCTION

The hippocampal formation, a circuit made up of interconnected subregions, plays a vital role in memory. Each hippocampal subregion houses a population of neurons with distinct molecular expression profiles and physiological properties. This molecular and functional anatomy is thought to account in part for the differential vulnerability of hippocampal subregions to various pathogenic mechanisms (1).

Indeed, although both Alzheimer's disease (AD) and the normal aging process affect hippocampal-dependent memory processes, several recent studies suggest that the two disorders might be distinguished by distinct anatomical patterns of hippocampal dysfunction (1). Postmortem studies have suggested that the entorhinal cortex (EC) as well as the CA1 subregion and the subiculum are the hippocampal subregions that are most affected by AD (2, 3), whereas the dentate gyrus (DG) and CA3 are relatively preserved (2, 4, 5). Similar patterns have been detected in vivo by high-resolution variants of functional magnetic resonance imaging (fMRI) (6–8). In contrast to AD, normal aging does not cause cell death or other pathognomonic histological abnormalities. Rather, age-related memory loss is characterized by dysfunctional neurons, and therefore, functional endpoints are best suited for mapping age-related hippocampal dysfunction. Results from high-resolution fMRI (7, 9, 10) and cognitive studies (11–14) suggest that the primary initial target of normal aging is the DG, whereas the EC is relatively preserved (1).

Although these anatomical patterns are suggestive, no specific molecular defects underlying age-related DG dysfunction have been identified. To obtain more direct evidence that age-related memory loss is not an early form of AD, we sought to isolate a molecular correlate of the aging human DG and explore whether this molecule mediates age-related memory loss. We hoped that these experiments could achieve two goals. First, the results could confirm or deny the anatomical pattern associated with aging and therefore further establish that aging and AD target the hippocampal circuit via separate mechanisms. Second, these findings could offer insight into the etiology of age-related memory loss with the potential of opening up new therapeutic avenues.

Although well suited to screen for molecular correlates of aging, gene expression profiling presents analytic challenges when applied to tissue harvested from postmortem human brain. Unlike the controlled experimental setting of animal models, the many genetic and life-style differences between human subjects affect expression levels independent of age and are therefore considered sources of variance. As described (15), one approach to addressing this challenge is to normalize expression levels to a region unaffected by aging, thereby reducing sources of variance. Guided by the image studies reviewed above, we used expression levels in the EC to normalize expression in the DG. In so doing, we identified 17 candidate aging-

associated genes and focused on one, RbAp48, whose decline in expression best correlated with the aging human DG. We then turned to mouse models and used cognitive, fMRI, and molecular analyses to examine the role of RbAp48 in age-related hippocampal dysfunction in the DG.

RESULTS

RbAp48 deficiency in the aging human hippocampus

Guided by the spatiotemporal pattern that distinguishes age-related hippocampal dysfunction from AD, we harvested the DG from postmortem human brains that were free of any detectable brain pathology, ranging in age from 33 to 88. In addition, we harvested from each brain the EC, as a within-brain control. Gene expression profiles were generated with Affymetrix microarray chips (one microarray per individual and brain area). We performed a hypothesis-driven analysis (15, 16) on the basis of the observation that the DG is preferentially affected by aging, whereas the EC is relatively spared. We first normalized expression levels of genes in the DG to their expression in the EC; the normalized values for the DG transcripts were then assessed for correlation with age of the subject. We found 17 normalized transcripts that decreased or increased with age, with $P \leq 0.005$. We verified that the changes in these normalized transcripts were not a result of age-associated changes in their abundance in the EC (Table 1 and fig. S1). One of the genes with the largest expression change also had values that conformed to the spatiotemporal pattern of normal age-related hippocampal dysfunction. This gene encoded RbAp48, a transcriptional regulator ($\beta = -0.94$, $P = 0.0005$) (Fig. 1, A and C).

We therefore focused on *RbAp48* and carried out an independent analysis of age-related changes in the protein encoded by this gene. We harvested the EC and DG as well as additional hippocampal subregions (CA3, CA1, and subiculum) from a separate group of 10 healthy human brains, ranging from 41 to 89 years of age (Fig. 1C). Using Western blots, we measured RbAp48 and actin in each tissue sample. As for the mRNA, the amount of RbAp48 protein declined with age in the DG ($\beta = -0.72$, $P = 0.02$), but not in the EC ($\beta = 0.13$, $P = 0.71$) (Fig. 1, B and D) or other hippocampal subregions (CA3: $\beta = 0.09$, $P = 0.81$; CA1: $\beta = -0.48$, $P = 0.16$; subiculum: $\beta = 0.12$, $P = 0.62$).

A forebrain-specific, dominant-negative inhibitor of RbAp48 in mice

RbAp48 plays multiples roles in histone acetylation and transcriptional regulation. It is also implicated in the cyclic adenosine monophosphate (cAMP)–protein kinase A (PKA)–cAMP response element–binding protein 1 (CREB1) pathway (17). Histone acetylation and the cAMP-PKA-CREB1 pathway are both required for normal hippocampal function and aging in the mouse (18–23). We therefore further investigated RbAp48 and tested whether its modulation could cause age-related memory decline in mice.

In wild-type mice, RbAp48 was expressed at high levels in the hippocampus, particularly in the DG (Fig. 2A). Consistent with our findings in humans, RbAp48 protein was less abundant in the DG of aged mice than in the DG of young mice. This age-related reduction

of RbAp48 was selective to the DG; its abundance in the CA3-CA1 subregion of the hippocampus was similar in aged and young mice (Fig. 2B).

To examine the function of RbAp48, we generated double-transgenic (DT) mice that expressed a dominant-negative form of RbAp48 (henceforth RbAp48-DN). This form of RbAp48 lacked the first 54 N-terminal amino acid residues, which are critical for the interaction of RbAp48 with histone H4, but retained the ability to bind to histone modification factors through the WD40 repeats (24). We restricted the expression of RbAp48-DN to the forebrain by using the CaMKIIα promoter and controlled its expression temporally with the tTA system (25) (Fig. 2C). This approach allowed us to inhibit RbAp48 function in the adult forebrain of DT mice in a spatially restricted and reversible manner. To discriminate between the endogenous and the recombinant RbAp48 proteins, we fused a Flag epitope tag to the N terminus of RbAp48-DN. To avoid developmental effects, we inhibited *RbAp48*-DN transcription in DT mice until day P40 with doxycycline (Fig. 2C). When we stopped doxycycline treatment to mice at day P40 and examined them at day P95 (adults), consistent with its anticipated dominant-negative function, RbAp48-DN in DT mice colocalized with endogenous RbAp48 in hippocampal neurons and significantly reduced the binding of RbAp48 to H4 compared to that in control siblings (Fig. 2, D and E).

Effect of forebrain-specific inhibition of RbAp48 on memory in young mice

We next asked whether inhibiting RbAp48 in the young adult mouse (3.5 months) forebrain interferes with memory. Because differences in anxiety can affect cognitive performance, we first examined all groups of mice on the elevated plus maze and in the open field. The elevated plus maze is widely used to measure anxiety for rodents. The basic measure of this task is the animals' preference for dark over exposed places. In the open field, mice with anxiety-like phenotypes avoid the center of the arena. The two groups, whether with inhibited RbAp48 (experimental) or functional RbAp48 (control), performed similarly in both tasks (fig. S2A). Thus, we concluded that anxiety levels are similar in the DT and the control mice and that differences in anxiety levels would not confound interpretation of results from our cognitive tasks.

We then tested for hippocampal-dependent dysfunction with a novel object recognition task. Unlike other rodent tasks, novel objection recognition–type tasks are valid in numerous mammalian species, and indeed, an age-related decline in novel object recognition has been documented in humans (26–28), as well as in animal models (29–31). We used a single-trial familiarization (training) protocol (32), which is hippocampus-dependent (33). The mice were placed in an open arena containing two identical objects and were allowed to explore them for 15 min. Independent of genotype, the mice explored both objects equally (Fig. 3A). Twenty-four hours after the training session, the animals were placed back in the arena, where one familiar and one novel object were presented. Control and DT mice displayed similar performance, that is, both groups exhibited a strong preference for the novel object, indicating that they retained a good memory of the familiar object after 24 hours (Fig. 3A). We found, however, that the memory of the novel object formed by the DT mice was significantly less robust than that formed by their control siblings, as evidenced by a memory test that we gave the mice 1 day later (48 hours after the initial familiarization

session). At 48 hours, the DT mice explored both objects equally, whereas the control mice again displayed a large preference for the novel object (Fig. 3A). To confirm that the poor performance of the DT mice in the 48-hour memory test was not a result of enhanced extinction learning (because the novel and familiar objects were the same in the 24-and 48-hour tests), we subjected another group of animals to a shorter initial familiarization session (10 min instead of 15 min). With this shorter training protocol, the DT mice did not remember the familiar object 24 hours later, whereas the control mice had formed a good memory at 24 hours (Fig. 3A and fig. S2B). Because no other memory test was performed before the 24-hour memory test, an extinction-related effect cannot have contributed to the low performance of the DT mice. These data suggest that inhibition of RbAp48 in the forebrain of young mice results in compromised novel object recognition memory.

The tTA system allowed us to confirm that the memory deficit in the DT mice resulted from acute action of RbAp48-DN in mature adult forebrain neurons and not from an early compensatory effect secondary to its expression between the day of its activation (day P40) and adulthood or to a positional effect of the transgene. DT mice and control littermates remained on doxycycline-containing food until day P40, at which point they were switched to doxycycline-free food, allowing synthesis of RbAp48-DN. Forty days later (day P80), the mice were shifted back to doxycycline-containing food, blocking the expression of RbAp48-DN (Fig. 2C). At day P105 (3.5 months), the mice were tested in the novel object recognition task. The DT and control mice on doxycycline performed similarly (Fig. 3B and fig. S2, C and D), indicating that when RbAp48-DN expression was eliminated in the adult forebrain of DT mice (that is, DT mice were fed doxycycline) and the inhibition of RbAp48 was released, these mice retained the ability to recognize novel objects. Thus, the compromised novel object recognition memory in DT mice expressing RbAp48-DN results from acute inhibition of RbAp48 by RbAp48-DN in adult forebrain neurons.

Because RbAp48 is involved in the control of cell cycle and proliferation (34, 35), we examined whether the impaired memory in RbAp48-DN DT mice could be due to altered neurogenesis in the hippocampus. We measured neurogenesis by performing immunohistochemistry and counting the numbers of cells expressing Ki67, a marker of proliferation, and DCX, a marker of developing newborn neurons, in the DG of 4-month-old DT and control mice (Fig. 3C). We found no differences in cell numbers between DT and control mice, indicating that neurogenesis is not affected in the hippocampus of DT animals. In addition, the memory of these mice returned to normal when they were switched to doxycycline-containing food in adulthood, showing that the memory deficits did not result from defective neurogenesis-related mechanisms.

We next examined the performance of the mice in the Morris water maze (36), a spatial memory task. Although this task can be performed normally by mice with subtle molecular defects in the DG, selective lesions of the DG cause memory impairment as measured by this task (37). The DT mice learned the task as well as their control siblings, as evident by their similar path lengths and escape latencies (time to find the platform) during the acquisition phase (Fig. 4A and fig. S4A). However, 1 day after the end of the acquisition phase, DT mice showed impaired memory; they exhibited a significant decrease in the number of times they crossed the location of the platform during a probe trial (Fig. 4A).

Comparison of noncognitive parameters (swim speed, floating, and thigmotaxis) revealed no differences between the groups (fig. S5). We also tested the mice in the transfer phase of the hidden platform version of the water maze. In this test, the platform was moved to the opposite quadrant, and the mice were tested for their ability to learn and remember the new platform location. Again, the DT mice had difficulty in forming a good memory of the new platform location; they explored the new training quadrant and crossed the platform location significantly less often than did the control animals in a probe trial 1 day after the end of training (Fig. 4A and fig. S4A). Control and DT animals on doxycycline (to inhibit transgene expression) showed no differences in the number of platform crossings (Fig. 4B and figs. S4B and S6).

Memory deficits in RbAp48-DN mice and aged wild-type mice

We then tested whether the memory deficits in the young RbAp48-DN mice were similar to those seen in aged wild-type animals. We compared young (3.5 months) and aged (15 months) wild-type mice with genetic backgrounds similar to those of RbAp48-DN animals (50% C57BL/6J and 50% 129SvEvTac). Aged mice displayed memory deficits for novel object recognition that were similar to those observed in young RbAp48-DN animals (Fig. 3D; anxiety tests: fig. S3, A to C). In the Morris water maze, the aged mice displayed higher escape latencies than did young mice during training (that is, the aged mice needed more time to find the platform), but this was likely due to their lower swimming speed (figs. S4C and S7) (38, 39), because the path lengths were similar between the two groups of animals (Fig. 4C). In addition, by the end of training, the latencies of the aged mice had significantly decreased and reached a plateau, indicating that they learned the platform locations (fig. S4C). These data indicate that aged mice with genetic backgrounds similar to that of RbAp48-DN mice learned the platform locations in the Morris water maze as well as young animals. The aged mice, however, did not form a robust memory of the platform location in either the hidden or the transfer phase because they performed significantly worse than young mice during the probe trials (Fig. 4C and fig. S4C). Together, our data indicate that inhibition of RbAp48 in the forebrain of young (3.5 months) adult mice recapitulates cognitive defects characteristic of hippocampal aging in mice with similar genetic background.

Effects of RbAp48-DN in the DG

We reasoned that if RbAp48 deficiency underlies age-related hippocampal dysfunction, inhibiting RbAp48 in young mice (3.5 months) should recapitulate the preferential dysfunction of the DG observed by fMRI in elderly mice, rhesus monkeys, and people (7, 9, 10). To explore this idea, we used a variant of fMRI that maps regional cerebral blood volume (CBV), a hemodynamic correlate of metabolism that generates functional maps with high spatial resolution (8, 40) and that can pinpoint regional dysfunction within the hippocampus in mouse models (9, 41–43). Compared to control mice, mice expressing RbAp48-DN exhibited selective dysfunction in the DG (Fig. 5A). This dysfunction was reversed when the expression of RbAp48-DN was turned off in the adult forebrain by feeding the DT mice with doxycycline-containing food (Fig. 5A).

Effect of RbAp48-DN expression on histone acetylation in the DG

Because RbAp48 regulates histone acetylation, we explored whether RbAp48-DN affects steady-state histone acetylation using immunohistochemistry and image quantification analysis. Guided by our gene expression and fMRI findings, we initially focused on the DG and examined the acetylation of H4(Lys^{12}) and H2B(Lys^{20}). RbAp48 interacts with H4 (24), and AcH4(Lys^{12}) is associated with age-related hippocampal dysfunction and memory loss in mice (23). RbAp48 also interacts with the phospho-CREB1–CBP (CREB-binding protein) complex and regulates the histone acetyltransferase (HAT) activity of CBP (17), and H2B(Lys^{20}) is a target of CBP (44, 45). By comparing the DG of RbAp48-DN mice to controls, we found that inhibition of RbAp48 caused a reduction in acetylation of both H4(Lys^{12}) and H2B (Lys^{20}) (Fig. 5B). We also examined AcH3(Lys^{9}), which is not involved in memory processes and not affected in the aged hippocampus (23), and found that AcH3(Lys^{9}) was not altered in the DG of RbAp48-DN mice (Fig. 5C). To test for spatial specificity of these effects, we examined the CA1 subregion of the hippocampus and found no significant reduction in histone acetylation (Fig. 5, B and C). As with behavior and fMRI, the effect of RbAp48-DN on AcH2B(Lys^{20}) and AcH4(Lys^{12}) in the adult DG was reversed when its expression was turned off (Fig. 5B).

Effect on memory of up-regulation of RbAp48 in the aged DG

Our data suggest that RbAp48 contributes to the DG-dependent molecular processes underlying memory function. If RbAp48 deficiency in the DG is linked to age-related deficits of hippocampus-dependent memory, then up-regulating RbAp48 in the DG of aged mice would ameliorate these deficits. Indeed, increasing RbAp48 in the DG of aged mice through lentiviral gene transfer (achieving a ~67% increase in protein abundance; Fig. 6A) significantly improved memory performance in both the novel object recognition and Morris water maze tasks (Fig. 6B and figs. S3D and S8) to a value comparable to that of wild-type young mice (compared with Figs. 3D and 4C). The improved memory was accompanied by an increase in the amount of AcH2B(Lys^{20}) and AcH4(Lys^{12}), but not AcH3 (Lys^{9}), in the DG, consistent with our findings in RbAp48-DN mice (Fig. 6C).

The two forms of memory that improve with up-regulation of RbAp48 in the aged DG, namely, novel object recognition memory and spatial reference memory, are unaffected when neurogenesis is increased in the DG (46), consistent with a role of RbAp48 in memory and age-related memory loss independent of neurogenesis.

Effect of RbAp48-DN expression in the forebrain on HAT activity of CBP

RbAp48 interacts with CREB1-dependent CBP and regulates its HAT activity (17), which is a critical component of memory (19). We therefore asked whether inhibiting RbAp48 in the young adult forebrain affects the HAT activity of CBP, and if so, whether such an effect occurs in aged mice. By carrying out CBP-specific immunoprecipitation from adult DG and CA3-CA1 protein lysates and then HAT assays, we found that the CBP HAT activity, but not the amount of CBP protein, was significantly lower in the DG of RbAp48-DN–expressing mice than in controls, whereas it was unaltered in the CA3-CA1 (Fig. 7A and fig. S9A). Selective reduction of CBP HAT activity in the DG was also observed in aged wild-type

mice, which was rescued upon lentivirus-mediated DG-specific up-regulation of RbAp48 (Fig. 7, B and C, and fig. S9, B and C).

Take together, our data demonstrate that RbAp48 plays an important role in hippocampus-related memory processes, and suggest a causal role of RbAp48 in cognitive aging.

DISCUSSION

This investigation provides more direct and causal evidence for a fundamental difference between age-related memory loss and AD. We performed a microarray screen in the human DG, using expression levels in the EC to normalize the data and control for interindividual expression differences not related to aging. We identified age-related changes in 17 transcripts and focused on one, an age-related decline in RbAp48, a molecule that previous studies have found to regulate histone acetylation and to interact with CBP (17). Because of the relatively low number of brains examined, we cannot rule out false-negative findings, and therefore, our analysis does not exclude the importance of genes found in other studies or in other regions (47). To explore the significance of RbAp48, we tested whether its expression also declines in aging wild-type mice and found a DG-selective deficiency in RbAp48 similar to that in human DG. These data indicate that an RbAp48 deficiency occurs in both the rodent and human DG in association with normal aging.

To further explore the significance of this finding, we turned to genetically engineered mice and validated that RbAp48 plays a causal role in driving age-related memory loss. We found that selective inhibition of RbAp48 in the forebrain of young mice recapitulates the cognitive and fMRI defects characteristic of hippocampal aging. Confirming RbAp48's known role, we found that inhibition of RbAp48 caused a reduction in histone acetylation and that the effect was selective to the DG. The decrease in H4(Lys^{12}) acetylation is in agreement with its recently identified association with age-dependent memory impairment in mice (23). The reduction of H2B(Lys^{20}) acetylation is particularly interesting because previous studies in our laboratory have found that a deficiency in CBP causes Rubinstein-Taybi syndrome and is associated with a decrease in H2B acetylation and hippocampal dysfunction (18). Indeed, RbAp48 interacts with CREB1-dependent CBP and regulates its HAT activity (17), a critical component in both explicit and implicit memory storage (19). Consistent with these findings, we saw DG-specific reduction of the HAT activity of CBP in the RbAp48-DN mice as well as in wild-type aged animals. Remarkably, increasing RbAp48 abundance in the DG of aged mice reversed these effects, and this was accompanied by improved memory performance.

Our results suggest that RbAp48 activity is necessary in the DG for proper hippocampal function. Indeed, although we expressed RbAp48-DN in all hippocampal subregions, the presence of this dominant-negative form of the protein only affected the CBV and histone acetylation mechanisms in the DG. This regional specificity could be explained by the distinct molecular anatomy of hippocampal subregions, which may confer differential sensitivity to molecular changes. The observed DG-specific effects of RbAp48-DN might reflect a preferential vulnerability of memory processes in the DG to RbAp48 deficiency and indicate that its decline with age contributes to age-related hippocampal-based memory loss.

Our demonstration that up-regulation of RbAp48 in the aging DG ameliorated age-related hippocampal-dependent memory deficits supports this idea.

Together, our results have a number of implications. The specific deficiency of RbAp48 in the human hippocampal formation with age is consistent with earlier imaging studies showing age-associated patterns of hippocampal vulnerability. The validation in normal and in genetically engineered mice that RbAp48 plays a role in hippocampal-dependent memory and age-related memory loss confirms that this selective pattern occurs in people. By extension, our studies support the idea that age-related memory loss is a disorder independent of AD. Furthermore, because RbAp48 has not been implicated in previous AD studies, our findings provide further evidence that hippocampal dysfunction in AD and aging are driven by distinct pathogenic mechanisms.

Finally, our data suggest that RbAp48 mediates its effects, at least in part, through the PKA-CREB1-CBP pathway, which we have earlier identified as being important for age-related memory loss in the mouse (48). This molecule and the PKA-CREB1-CBP pathway are therefore valid targets for therapeutic intervention. It has already been shown that agents that enhance the PKA-CREB1 pathway ameliorate age-related hippocampal dysfunction in rodents (48). Our results suggest that CREB1-enhancing drugs may have similar beneficial effects in aging humans.

MATERIALS AND METHODS

Study design

To identify molecular defects underlying age-related memory loss, we carried out a gene expression study on human postmortem tissue, free of histopathology. We examined expression in the DG, the subregion of the hippocampal formation thought to be the site of onset of age-related memory loss, and used as normalizer expression in the EC, a neighboring subregion unaffected by aging and known to be the site of onset of AD. We further explored the gene that showed the largest change limited to the DG and used mouse models to examine whether this change is causally linked to age-related memory loss.

The experimenter was blinded in all human and mouse studies. No outliers were detected or excluded. Male mice were used. In the transgenic mouse studies, the single tetO, single tTA, and wild-type (no transgene in the genome) control genotypes showed no differences and were pooled in the control group (table S3). On/off and on/off/on diet protocols were used in all studies. The mice were selected by a person not involved in the experiments, and in such a way that all genotypes, ages, and treatments were similarly represented in the experiments. Behavioral tasks were performed once for each group of mice. Behaviorally tested, virus-injected animals were analyzed after the end of testing for the success of the injections by immunostaining and the following criteria: (i) specificity for DG and (ii) successful injections in both hemispheres. Mice that did not meet these criteria were excluded from the analysis. For histone acetylation and HAT assays, a different group of mice was used. Similar selection criteria were followed. For histone acetylation assays, the selection was made with immunohistochemistry, whereas for HAT assays, it was made with Western blot analysis of a fraction of the protein lysates used for the assays.

Human gene expression profiling

Eight brains, free of histopathology, were obtained at autopsy under a protocol approved by Columbia University's review board. The DG and EC were identified and sectioned with strict anatomical criteria, following the New York Brain Bank procedures. Total RNA was extracted with TRIzol and RNeasy column (Invitrogen). RNA (10 μg) and T7-$(dT)_{24}$ primer were used for double-stranded complementary DNA (cDNA) synthesis (SuperScript, Invitrogen). In vitro transcription with biotin-labeled ribonucleotides produced complementary RNA (cRNA) probes (ENZO Life Sciences; ENZ-42655-40). HG-U133A Affymetrix microarrays were hybridized with fragmented cRNA for 16 hours at 45°C with constant rotation (60*g*). Microarrays were analyzed with Affymetrix Mcroarray Suite v5.0 and GeneSpring v5.0.3 (Silicon Genetics) software, and scaled to a value of 500. Samples with a 3′/5′ ratio of control genes *ACTIN* and *GAPDH* greater than 7 were excluded from analysis. We excluded transcripts whose detection levels had a *P* value greater than 0.05, yielding a final data set of 6565 transcripts. Guided by a spatiotemporal pattern of hippocampal dysfunction that distinguishes aging from AD (15, 16), expression levels from the DG were normalized to levels in the EC and then correlated with age. In a secondary analysis, bivariate Pearson's correlations were performed for transcripts of interest within each the DG and EC, and transcripts that showed a significant age-associated effect in the EC were removed from the final list of "hits" (Table 1).

Western blot analysis

Human hippocampal subsections were lysed in 20 mM tris-HCl (pH 7.9), 150 mM NaCl, 5% NP-40, 1 mM EDTA, 10 mM 4-(2-aminoethyl) benzenesulfonyl fluoride (AEBSF), and Protease Inhibitor Mixture (Roche). Mouse hippocampi and subregions were lysed in 50 mM tris-HCl (pH 7.4) and 2% SDS buffer. Ten to 20 μg (mouse) and 40 μg (human) of lysates were separated by SDS-polyacrylamide gel electrophoresis and transferred to polyvinylidene difluoride membranes (Bio-Rad). Membranes were blocked in 5% milk in 50 mM tris-HCl (pH 7.4), 0.9% NaCl, and 0.1% Tween 20. In human studies, immunoblots were analyzed with the Odyssey Infrared Imaging System (LI-COR Biosciences). In mouse studies, SuperSignal (Pierce) and ECL Plus reagents (Amersham) were used for visualization; the ImageQuant software was used for quantification. Anti-RbAp48 antibodies were from GeneTex (GTX70232) and Thermo Scientific (PA1-869). Anti-Flag antibody was from Sigma (F3165).

Generation of transgenic mice

The *Flag-RbAp48-DN* coding sequence was amplified by polymerase chain reaction (PCR) and subcloned into the pMM400 plasmid (32) (see table S2 for the oligonucleotides used for the PCR cloning). Linearized *tetO–Flag–RbAp48-DN* transgene was injected into pronuclei of one-cell C57BL/6-CBA(J) F2 oocytes, which were transferred via the oviduct into pseudopregnant foster females. Founder animals were genotyped with Southern blots for *tetO*.

Maintenance and genetic background of mice

Mice were maintained under standard conditions approved by the Institutional Animal Care and Use Committee. To control for genetic background, we followed the recommendations made by the Banbury conference on genetic background in mutant mice (49). The *tetO–Flag–RbAp48-DN* mice (backcrossed at least six times to C57BL/6J background) were bred with *CaMKIIα-tTA* mice (backcrossed 16 to 18 times to 129SvEvTac background). Offspring were genotyped with Southern blots for *tetO* and *tTA*. For regulating *tetO*-driven gene expression, mice were fed chow supplemented with doxycycline (40 mg/kg) (Mutual Pharmaceutical). Wild-type mice used in our experiments also were F1 hybrids (50% C57BL/6J and 50% 129SvEvTac).

Radioactive RNA in situ hybridization

Radioactive RNA in situ hybridization was performed as described (32). After hybridization, the brain slices were dehydrated and exposed on x-ray film for 2 weeks. See table S2 for oligonucleotide/probe sequences.

Reverse transcription polymerase chain reaction

Reverse transcription PCR was performed as described (32). To clone the mouse RbAp48 cDNA, we subjected 5% of reverse transcriptase to 35 PCR cycles with RbAp48-sprecific primers (table S2).

HAT assays

Kit from Millipore was used (17–284). Anti-CBP antibody (Santa Cruz Biotechnology; sc-7300) was used for the immunoprecipitations (6 μg). DG (400 μg) and CA3-CA1 clear lysates (800 μg) (supernatants after centrifugation at 14,000 rpm for 10 min) were used as immunoprecipitation input.

Immunohistochemistry

Immunohistochemistry was performed as described (32). Anti-acH2B(Lys^{20}), anti-acH3(Lys^{9}), and anti-acH4(Lys^{12}) antibodies were from Cell Signaling Technology (2571, 9671, and 2591, respectively). The MetaMorph software (Molecular Devices) was used for quantification. For DCX (Millipore; AB2253), NeuN (Millipore; MAB377), and Ki67 (Abcam; ab15580) immunohistochemistry, serial coronal sections (30 μm) along the entire rostrocaudal extension of the hippocampus were cut on a vibratome and stored in 0.1 M tris (pH 7.4), 30% ethylene glycol, and 30% glycerol at −20°C until further processed. Immunohistochemistry was performed on every fifth section, starting from −1.58 mm from bregma.

Behavior

The behavioral tasks have been described (32). The elevated plus maze data were evaluated with ANOVA, with the genotype as the between factor and the arm (open and enclosed) as the within factor. ANOVA with the genotype as the between factor and the center of the arena as the within factor was used for the analysis of the open field data. The Morris water maze consisted of three phases: (i) 2 days of the mouse searching for a visible platform (four

trials per day), (ii) 8 days with a hidden platform in quadrant 3 (one trial per day; 4 days per week), and (iii) 8 days with the hidden platform in quadrant 1 (one trial per day; 4 days per week). Probe trials lasted 1 min. Statistical analyses used ANOVAs with genotype as the between-subject factor and day or area (quadrant or crossing during the probe trials) as the within-subject factor. In the novel object recognition, the mice were habituated in the arena for 15 min for three consecutive days. On the following day, the training session lasted 10 or 15 min. Testing phases lasted 5 min. The same novel and familiar objects were used in all tests. The discrimination index was determined by the difference in exploration time expressed as a ratio of the total time spent exploring the two objects.

Functional magnetic resonance imaging

Mice images were acquired with a Bruker AVANCE 400WB spectrometer outfitted with an 89-mm-bore, 9.4-T vertical Bruker magnet (Oxford Instruments Ltd.), a 30–mm–inside diameter birdcage RF probe, and a shielded gradient system (100 G/cm) before and 37.5 min after intraperitoneal injections of the contrast agent gadolinium (10 mmol/kg). As previously described (8), CBV maps were derived from gadolinium-enhanced T2-weighted images acquired with a fast-spin echo acquisition (time to repeat, 2000 ms; time to echo, 70 ms; in-plane resolution, 86 μm; slice thickness, 500 μm).

Lentiviral injections in the DG

The HA-RbAp48 cDNA was subcloned into the pFUGW-GFP plasmid (Addgene; 14883), replacing the coding sequence of GFP. pFUGW-GFP was used for generating control lentiviruses. The lentivirus production has been described (32). Lentiviral aliquots (1.5 μl) (2×10^9 infectious units/ml) were injected into the DG (0.375 μl/min). Stereotactic coordinates were as follows: anteroposterior (−1.85 mm) and mediolateral (±1.25 mm) from bregma, and dorsoventral (−1.90 mm) from brain surface (Paxinos Mouse Brain Atlas). Fourteen-month-old mice were injected and subjected to behavioral tasks or HAT and histone acetylation assays 4 weeks later.

Statistics

Statistics were performed with IBM SPSS 19.0 (microarray and fMRI) and StatView (SAS Institute; all the other mouse studies) software. For microarray analysis, the expression levels from the DG were normalized by levels in the EC and then correlated with age. Bivariate Pearson's correlations were performed for transcripts of interest within each region. For all the other studies, repeated-measures ANOVA, ANOVA, and *t* tests were used as indicated. Scheffé test was the post hoc analysis. The results are presented as means ± SEM. Statistical significance was set at $P < 0.05$.

Supplementary Material

Refer to Web version on PubMed Central for supplementary material.

Acknowledgments

We thank E. Simpson and C. Kellendonk for their critical comments, and K. Hess and F. Hau for technical help.

Funding: The work was supported by the Howard Hughes Medical Institute, the James S. McDonnell Foundation, the Broitman Foundation, the Henry M. Jackson Foundation, and the NIH/National Institute on Aging grant AG034618.

REFERENCES AND NOTES

1. Small SA, Schobel SA, Buxton RB, Witter MP, Barnes CA. A pathophysiological framework of hippocampal dysfunction in ageing and disease. Nat Rev Neurosci. 2011; 12:585–601. [PubMed: 21897434]
2. Braak H, Alafuzoff I, Arzberger T, Kretzschmar H, Del Tredici K. Staging of Alzheimer disease-associated neurofibrillary pathology using paraffin sections and immunocytochemistry. Acta Neuropathol. 2006; 112:389–404. [PubMed: 16906426]
3. Gómez-Isla T, Price JL, McKeel DW Jr, Morris JC, Growdon JH, Hyman BT. Profound loss of layer II entorhinal cortex neurons occurs in very mild Alzheimer's disease. J Neurosci. 1996; 16:4491–4500. [PubMed: 8699259]
4. Thal DR, Rüb U, Orantes M, Braak H. Phases of Aβ-deposition in the human brain and its relevance for the development of AD. Neurology. 2002; 58:1791–1800. [PubMed: 12084879]
5. West MJ. Regionally specific loss of neurons in the aging human hippocampus. Neurobiol Aging. 1993; 14:287–293. [PubMed: 8367010]
6. Small SA, Perera GM, DeLaPaz R, Mayeux R, Stern Y. Differential regional dysfunction of the hippocampal formation among elderly with memory decline and Alzheimer's disease. Ann Neurol. 1999; 45:466–472. [PubMed: 10211471]
7. Small SA, Tsai WY, DeLaPaz R, Mayeux R, Stern Y. Imaging hippocampal function across the human life span: Is memory decline normal or not? Ann Neurol. 2002; 51:290–295. [PubMed: 11891823]
8. Moreno H, Hua F, Brown T, Small S. Longitudinal mapping of mouse cerebral blood volume with MRI. NMR Biomed. 2006; 19:535–543. [PubMed: 16552789]
9. Moreno H, Wu WE, Lee T, Brickman A, Mayeux R, Brown TR, Small SA. Imaging the Aβ-related neurotoxicity of Alzheimer disease. Arch Neurol. 2007; 64:1467–1477. [PubMed: 17923630]
10. Small SA, Chawla MK, Buonocore M, Rapp PR, Barnes CA. Imaging correlates of brain function in monkeys and rats isolates a hippocampal subregion differentially vulnerable to aging. Proc Natl Acad Sci USA. 2004; 101:7181–7186. [PubMed: 15118105]
11. Toner CK, Pirogovsky E, Kirwan CB, Gilbert PE. Visual object pattern separation deficits in nondemented older adults. Learn Mem. 2009; 16:338–342. [PubMed: 19403797]
12. Yassa MA, Lacy JW, Stark SM, Albert MS, Gallagher M, Stark CE. Pattern separation deficits associated with increased hippocampal CA3 and dentate gyrus activity in nondemented older adults. Hippocampus. 2011; 21:968–979. [PubMed: 20865732]
13. Stark SM, Yassa MA, Stark CE. Individual differences in spatial pattern separation performance associated with healthy aging in humans. Learn Mem. 2010; 17:284–288. [PubMed: 20495062]
14. Brickman AM, Stern Y, Small SA. Hippocampal subregions differentially associate with standardized memory tests. Hippocampus. 2011; 21:923–928. [PubMed: 20824727]
15. Lewandowski NM, Small SA. Brain microarray: Finding needles in molecular haystacks. J Neurosci. 2005; 25:10341–10346. [PubMed: 16280569]
16. Small SA, Kent K, Pierce A, Leung C, Kang MS, Okada H, Honig L, Vonsattel JP, Kim TW. Model-guided microarray implicates the retromer complex in Alzheimer's disease. Ann Neurol. 2005; 58:909–919. [PubMed: 16315276]
17. Zhang Q, Vo N, Goodman RH. Histone binding protein RbAp48 interacts with a complex of CREB binding protein and phosphorylated CREB. Mol Cell Biol. 2000; 20:4970–4978. [PubMed: 10866654]
18. Alarcón JM, Malleret G, Touzani K, Vronskaya S, Ishii S, Kandel ER, Barco A. Chromatin acetylation, memory, and LTP are impaired in $CBP^{+/-}$ mice: A model for the cognitive deficit in Rubinstein-Taybi syndrome and its amelioration. Neuron. 2004; 42:947–959. [PubMed: 15207239]

19. Korzus E, Rosenfeld MG, Mayford M. CBP histone acetyltransferase activity is a critical component of memory consolidation. Neuron. 2004; 42:961–972. [PubMed: 15207240]
20. Vecsey CG, Hawk JD, Lattal KM, Stein JM, Fabian SA, Attner MA, Cabrera SM, McDonough CB, Brindle PK, Abel T, Wood MA. Histone deacetylase inhibitors enhance memory and synaptic plasticity via CREB:CBP-dependent transcriptional activation. J Neurosci. 2007; 27:6128–6140. [PubMed: 17553985]
21. Chung YH, Kim EJ, Shin CM, Joo KM, Kim MJ, Woo HW, Cha CI. Age-related changes in CREB binding protein immunoreactivity in the cerebral cortex and hippocampus of rats. Brain Res. 2002; 956:312–318. [PubMed: 12445700]
22. Trompet S, Craen AJ, Jukema JW, Pons D, Slagboom PE, Kremer D, Bollen EL, Westendorp RG. Variation in the CBP gene involved in epigenetic control associates with cognitive function. Neurobiol Aging. 2011; 32:549.e541–549.e548. [PubMed: 20096957]
23. Peleg S, Sananbenesi F, Zovoilis A, Burkhardt S, Bahari-Javan S, Agis-Balboa RC, Cota P, Wittnam JL, Gogol-Doering A, Opitz L, Salinas-Riester G, Dettenhofer M, Kang H, Farinelli L, Chen W, Fischer A. Altered histone acetylation is associated with age-dependent memory impairment in mice. Science. 2010; 328:753–756. [PubMed: 20448184]
24. Vermaak D, Wade PA, Jones PL, Shi YB, Wolffe AP. Functional analysis of the SIN3-histone deacetylase RPD3-RbAp48-histone H4 connection in the Xenopus oocyte. Mol Cell Biol. 1999; 19:5847–5860. [PubMed: 10454532]
25. Mayford M, Bach ME, Huang YY, Wang L, Hawkins RD, Kandel ER. Control of memory formation through regulated expression of a CaMKII transgene. Science. 1996; 274:1678–1683. [PubMed: 8939850]
26. Resnick SM, Trotman KM, Kawas C, Zonderman AB. Age-associated changes in specific errors on the Benton Visual Retention Test. J Gerontol B Psychol Sci Soc Sci. 1995; 50:171–178.
27. Schacter DL, Cooper LA, Valdiserri M. Implicit and explicit memory for novel visual objects in older and younger adults. Psychol Aging. 1992; 7:299–308. [PubMed: 1610519]
28. Grady CL, McIntosh AR, Horwitz B, Maisog JM, Ungerleider LG, Mentis MJ, Pietrini P, Schapiro MB, Haxby JV. Age-related reductions in human recognition memory due to impaired encoding. Science. 1995; 269:218–221. [PubMed: 7618082]
29. Moss MB, Rosene DL, Peters A. Effects of aging on visual recognition memory in the rhesus monkey. Neurobiol Aging. 1988; 9:495–502. [PubMed: 3062461]
30. Rapp PR, Amaral DG. Evidence for task-dependent memory dysfunction in the aged monkey. J Neurosci. 1989; 9:3568–3576. [PubMed: 2795141]
31. Erickson CA, Barnes CA. The neurobiology of memory changes in normal aging. Exp Gerontol. 2003; 38:61–69. [PubMed: 12543262]
32. Pavlopoulos E, Trifilieff P, Chevaleyre V, Fioriti L, Zairis S, Pagano A, Malleret G, Kandel ER. Neuralized1 activates CPEB3: A function for nonproteolytic ubiquitin in synaptic plasticity and memory storage. Cell. 2011; 147:1369–1383. [PubMed: 22153079]
33. Broadbent NJ, Gaskin S, Squire LR, Clark RE. Object recognition memory and the rodent hippocampus. Learn Mem. 2010; 17:5–11. [PubMed: 20028732]
34. Pacifico F, Paolillo M, Chiappetta G, Crescenzi E, Arena S, Scaloni A, Monaco M, Vascotto C, Tell G, Formisano S, Leonardi A. RbAp48 is a target of nuclear factor-κB activity in thyroid cancer. J Clin Endocrinol Metab. 2007; 92:1458–1466. [PubMed: 17244783]
35. Kong L, Yu XP, Bai XH, Zhang WF, Zhang Y, Zhao WM, Jia JH, Tang W, Zhou YB, Liu CJ. RbAp48 is a critical mediator controlling the transforming activity of human papillomavirus type 16 in cervical cancer. J Biol Chem. 2007; 282:26381–26391. [PubMed: 17616526]
36. Morris RG, Garrud P, Rawlins JN, O'Keefe J. Place navigation impaired in rats with hippocampal lesions. Nature. 1982; 297:681–683. [PubMed: 7088155]
37. Keith JR, Wu Y, Epp JR, Sutherland RJ. Fluoxetine and the dentate gyrus: Memory, recovery of function, and electrophysiology. Behav Pharmacol. 2007; 18:521–531. [PubMed: 17762521]
38. Sumien N, Sims MN, Taylor HJ, Forster MJ. Profiling psychomotor and cognitive aging in four-way cross mice. Age. 2006; 28:265–282. [PubMed: 22253494]

39. Verbitsky M, Yonan AL, Malleret G, Kandel ER, Gilliam TC, Pavlidis P. Altered hippocampal transcript profile accompanies an age-related spatial memory deficit in mice. Learn Mem. 2004; 11:253–260. [PubMed: 15169854]
40. Lin W, Celik A, Paczynski RP. Regional cerebral blood volume: A comparison of the dynamic imaging and the steady state methods. J Magn Reson Imaging. 1999; 9:44–52. [PubMed: 10030649]
41. Gaisler-Salomon I, Miller GM, Chuhma N, Lee S, Zhang H, Ghoddoussi F, Lewandowski N, Fairhurst S, Wang Y, Conjard-Duplany A, Masson J, Balsam P, Hen R, Arancio O, Galloway MP, Moore HM, Small SA, Rayport S. Glutaminase-deficient mice display hippocampal hypoactivity, insensitivity to pro-psychotic drugs and potentiated latent inhibition: Relevance to schizophrenia. Neuropsychopharmacology. 2009; 34:2305–2322. [PubMed: 19516252]
42. Wu W, Small SA. Imaging the earliest stages of Alzheimer's disease. Curr Alzheimer Res. 2006; 3:529–539. [PubMed: 17168652]
43. Chen YJ, Johnson MA, Lieberman MD, Goodchild RE, Schobel S, Lewandowski N, Rosoklija G, Liu RC, Gingrich JA, Small S, Moore H, Dwork AJ, Talmage DA, Role LW. Type III neuregulin-1 is required for normal sensorimotor gating, memory-related behaviors, and corticostriatal circuit components. J Neurosci. 2008; 28:6872–6883. [PubMed: 18596162]
44. Valor LM, Pulopulos MM, Jimenez-Minchan M, Olivares R, Lutz B, Barco A. Ablation of CBP in forebrain principal neurons causes modest memory and transcriptional defects and a dramatic reduction of histone acetylation but does not affect cell viability. J Neurosci. 2011; 31:1652–1663. [PubMed: 21289174]
45. Cvekl A, Duncan MK. Genetic and epigenetic mechanisms of gene regulation during lens development. Prog Retin Eye Res. 2007; 26:555–597. [PubMed: 17905638]
46. Sahay A, Scobie KN, Hill AS, O'Carroll CM, Kheirbek MA, Burghardt NS, Fenton AA, Dranovsky A, Hen R. Increasing adult hippocampal neurogenesis is sufficient to improve pattern separation. Nature 4. 2011; 72:466–470.
47. Berchtold NC, Cribbs DH, Coleman PD, Rogers J, Head E, Kim R, Beach T, Miller C, Troncoso J, Trojanowski JQ, Zielke HR, Cotman CW. Gene expression changes in the course of normal brain aging are sexually dimorphic. Proc Natl Acad Sci USA. 2008; 105:15605–15610. [PubMed: 18832152]
48. Bach ME, Barad M, Son H, Zhuo M, Lu YF, Shih R, Mansuy I, Hawkins RD, Kandel ER. Age-related defects in spatial memory are correlated with defects in the late phase of hippocampal long-term potentiation in vitro and are attenuated by drugs that enhance the cAMP signaling pathway. Proc Natl Acad Sci USA. 1999; 96:5280–5285. [PubMed: 10220457]
49. Silva AJ, Simpson EM, Takahashi JS, Lipp HP, Nakanishi S, Wehner JM, Giese KP, Tully T, Abel T, Chapman PF, Fox K, Grant S, Itohara S, Lathe R, Mayford M, McNamara JO, Morris RJ, Picciotto M, Roder J, Shin HS, Slesinger PA, Storm DR, Stryker MP, Tonegawa S, Wang Y, Wolfer DP. Mutant mice and neuroscience: Recommendations concerning genetic background. Banbury Conference on Genetic Background in Mice. Neuron. 1997; 19:755–759. [PubMed: 9354323]
50. Hawrylycz MJ, Lein ES, Guillozet-Bongaarts AL, Shen EH, Ng L, Miller JA, van de Lagemaat LN, Smith KA, Ebbert A, Riley ZL, Abajian C, Beckmann CF, Bernard A, Bertagnolli D, Boe AF, Cartagena PM, Chakravarty MM, Chapin M, Chong J, Dalley RA, Daly BD, Dang C, Datta S, Dee N, Dolbeare TA, Faber V, Feng D, Fowler DR, Goldy J, Gregor BW, Haradon Z, Haynor DR, Hohmann JG, Horvath S, Howard RE, Jeromin A, Jochim JM, Kinnunen M, Lau C, Lazarz ET, Lee C, Lemon TA, Li L, Li Y, Morris JA, Overly CC, Parker PD, Parry SE, Reding M, Royall JJ, Schulkin J, Sequeira PA, Slaughterbeck CR, Smith SC, Sodt AJ, Sunkin SM, Swanson BE, Vawter MP, Williams D, Wohnoutka P, Zielke HR, Geschwind DH, Hof PR, Smith SM, Koch C, Grant SG, Jones AR. An anatomically comprehensive atlas of the adult human brain transcriptome. Nature. 2012; 489:391–399. [PubMed: 22996553]

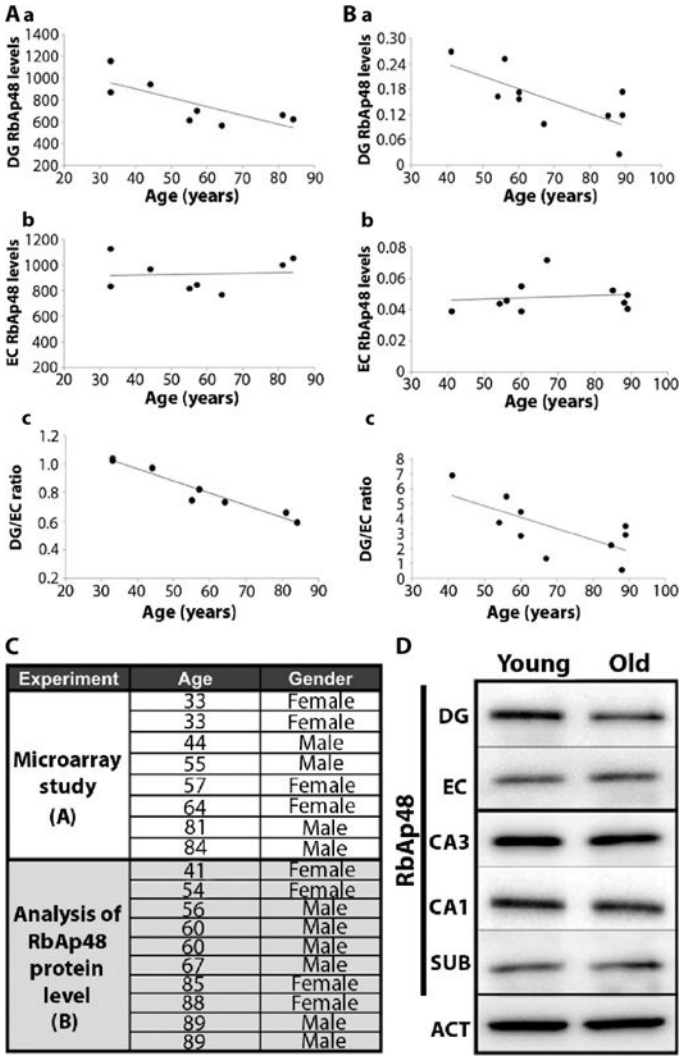

Experiment	Age	Gender
Microarray study (A)	33	Female
	33	Female
	44	Male
	55	Male
	57	Female
	64	Female
	81	Male
	84	Male
Analysis of RbAp48 protein level (B)	41	Female
	54	Female
	56	Male
	60	Male
	60	Male
	67	Male
	85	Female
	88	Female
	89	Male
	89	Male

Fig. 1. RbAp48 deficiency in the aging human hippocampal formation

(**A**) *RbAp48* gene expression over life span in (a) the DG showing a decline (β = −0.77, P = 0.026) and (b) the EC (β = 0.07, P = 0.87) showing no decline. (c) DG/EC ratio of RbAp48 declines with age (β = −0.94, P = 0.0005) (n = 8). (**B**) RbAp48 protein in separate group of brains (n = 10). RbAp48 protein levels decline over the life span (a) in the DG (β = −0.72, P = 0.02), but not (b) in the EC (β = 0.13, P = 0.71). (c) DG protein expression normalized to EC protein expression. In (A) and (B), each data point corresponds to one human subject and microarray experiment. (**C**) Human subjects used in the studies. (**D**) Representative Western blot showing RbAp48 levels in a young and an old sample. SUB, subiculum; ACT, actin (control; data from DG are shown).

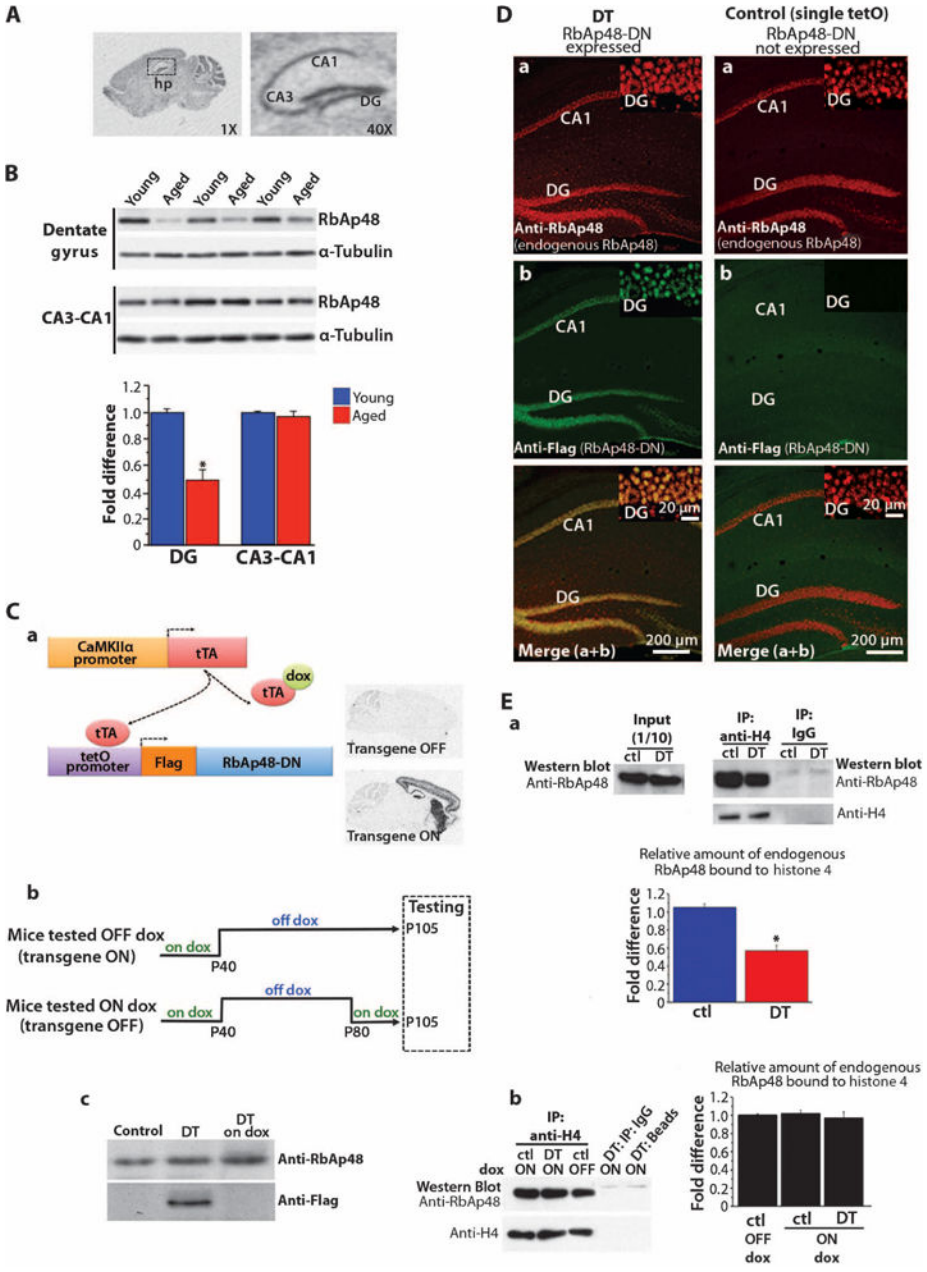

Fig. 2. Generation and characterization of DT mice expressing RbAp48-DN in the forebrain

(**A**) (Left) Radioactive in situ hybridization of *RbAp48* mRNA on a sagittal brain slice from adult wild-type (WT) mice (3.5 months). (Right) High magnification of left image showing *RbAp48* mRNA in the hippocampus (hp). See table S2 for hybridization probe sequence (oligo1). (**B**) Representative Western blot (different mouse in each lane) and averaged values below. RbAp48 values were normalized to tubulin values from the same mouse, and data from all mice were averaged and expressed as fold difference change in aged mice (15 months) compared to young mice (3.5 months) ± SEM. RbAp48 is reduced in the DG of aged mice compared to young mice ($*P = 3.2 \times 10^{-8}$). $n = 24$ per age (six mice per age; four independent experiments). (**C**) (a) Schematic representation of doxycycline (dox)–regulated

expression of Flag–RbAp48-DN in the forebrain. In DT mice that carried the *tetO*$_{promoter}$–*RbAp48-DN* and the *CaMKIIα*$_{promoter}$-*tTA* transgenes, the heterologous transactivator tTA bound to the *tetO* promoter and activated *RbAp48-DN* expression only in the forebrain where the *CaMKIIα* promoter is active. Maintaining the DT mice on doxycycline-containing food inhibits *RbAp48-DN* transcription because doxycycline prevents the binding of the tTA to the *tetO* promoter. (Right) *RbAp48-DN* mRNA in sagittal brain sections from adult (day P95) DT animals with no doxycycline treatment after day P40 (transgene ON; on/off dox diet) or with doxycycline treatment after day P80 to inhibit the transgene expression (transgene OFF; on/off/on dox diet). (b) Diet protocols for DT mice and control littermates used in all studies. (c) Western blot analysis of RbAp48-DN (anti-Flag) and endogenous RbAp48 in the hippocampus of 95-day-old mice. DT on dox, DT mouse treated with doxycycline (RbAp48-DN OFF); DT, mouse not fed with doxycycline in adulthood (RbAp48-DN ON); Control, *tetO–RbAp48-DN* single transgenic mouse. RbAp48-DN is detected only in DT. Four independent experiments gave similar results. (**D**) Confocal hippocampal images from adult (3.5 months) DT mouse and *tetO–RbAp48-DN* (*tetO*) single transgenic animal (control). (Insets) High-magnification DG images. (**E**) Binding of RbAp48 to histone 4 (H4). (a) Representative Western blots showing RbAp48 level in adult (3.5 months) hippocampal lysates before (input; left) and after (right) coimmunoprecipitation (IP) with anti-H4 antibody. Immunoprecipitated H4 is also shown (right). DT, RbAp48-DN–expressing mouse; ctl, control littermates. (b) Representative Western blots of immunoprecipitated H4 and coimmunoprecipitated RbAp48 from adult (3.5 months) hippocampal lysates from DT mice kept on doxycycline-containing food (RbAp48-DN OFF) and control littermates kept on or off dox in adulthood. IgG and beads: controls for the specificity of the anti-H4 immunoprecipitations. (Graphs) Averaged data (mean ± SEM). (a) DT: $n = 4$, ctl: $n = 6$ (tetO = 2, tTA = 2, WT = 2); (b) DT on dox: $n = 3$; ctl on dox: $n = 3$ (tetO = 1, tTA = 1, WT = 1). One experiment per mouse. The values of RbAp48 level after the anti-H4 immunoprecipitation were normalized to the H4 values from the same mouse, and data from all mice were averaged and expressed as fold difference change in DT compared to controls in (a) and fold difference change in DT on dox and controls on dox compared to controls off dox in (b). Significant difference was found between DT and controls in (a) [$*P = 2 \times 10^{-6}$, analysis of variance (ANOVA)].

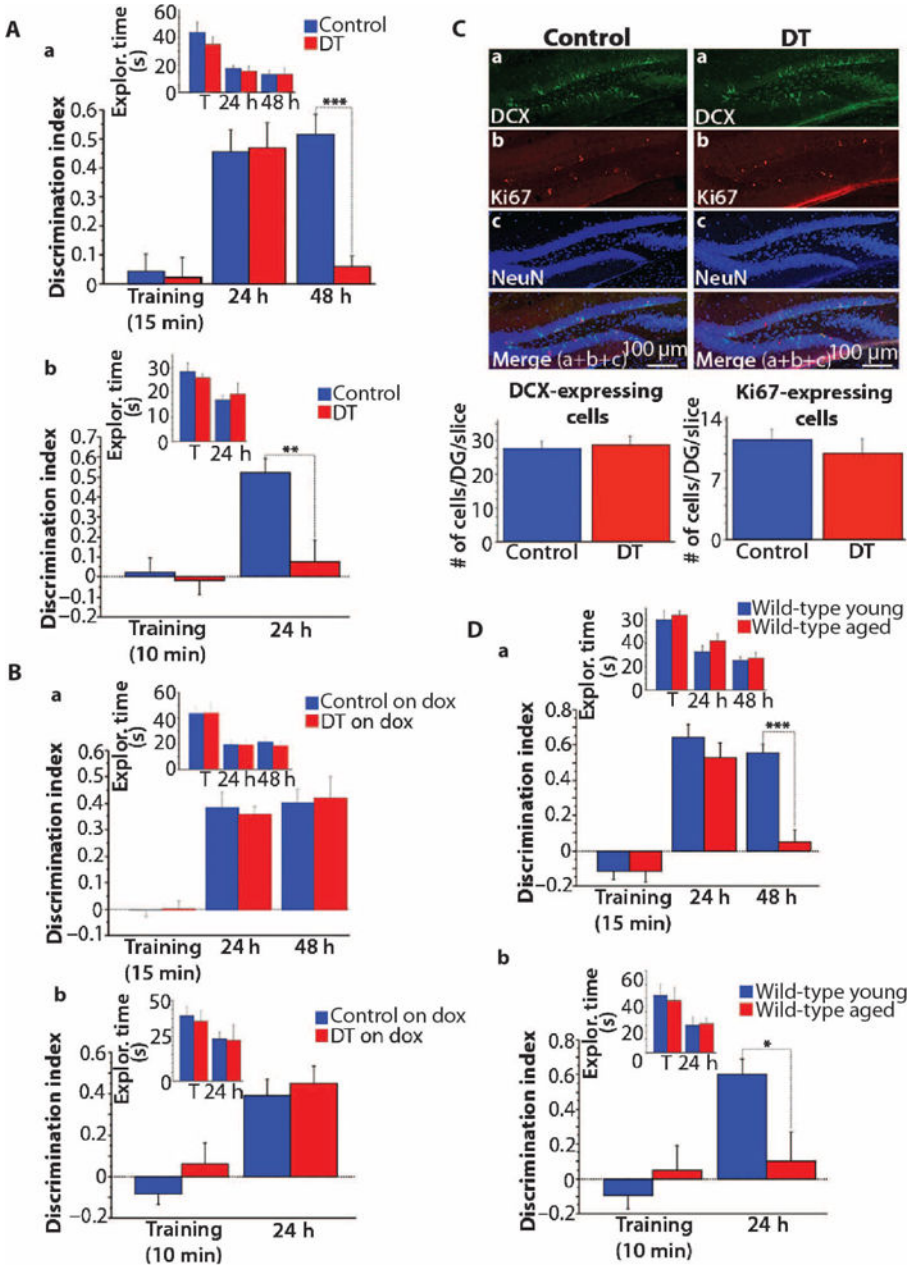

Fig. 3. Effect of RbAp48-DN in the adult forebrain on object recognition memory

Data from novel object recognition task (mean ± SEM; one experiment). (**A**) Mice kept off doxycycline during the task. (a) Fifteen-minute training [DT: $n = 11$; control: $n = 22$ (tetO = 6, tTA = 8, WT = 8)]. DT (RbAp48-DN ON) mice performed worse than did controls during the 48-hour memory test (genotype × test effect: $P = 0.0077$, repeated-measures ANOVA; $P = 0.0001$, t test). (b) Ten-minute training [different groups of mice; DT: $n = 12$; control: $n = 12$ (tetO = 5, tTA = 4, WT = 3)]. DT mice performed worse than did controls in the 24-hour memory test (genotype × test effect: $P = 0.0158$, repeated-measures ANOVA; $P = 0.0023$, t test). (**B**) Animals kept on doxycycline during the task (mean ± SEM; one experiment). (a) Fifteen-minute training [DT: n = 10; control: n = 17 (tetO = 5, tTA = 5, WT = 7)]. (b) Ten-

minute training [different groups; DT: $n = 12$; controls: $n = 21$ (tetO = 7, tTA = 7, WT = 7)]. DT on dox (*RbAp48-DN* OFF) and Control on dox displayed similar performance ($P > 0.2$, repeated-measures ANOVA). (**C**) Confocal images (30 μm) showing immunostaining against doublecortin (DCX) and Ki67 in the DG of 4-month-old RbAp48-DN–expressing (DT) and control mice. Graphs: Averaged data (±SEM). The numbers of DCX-and Ki67-expressing cells in DT and controls were similar ($P > 0.5$, ANOVA). DT: $n = 24$ (six mice; four slices per mouse) and controls: $n = 24$ [6 mice (tetO = 2, tTA = 2, WT = 2); four slices per mouse]. NeuN, marker of mature neurons. (**D**) Data from novel object recognition (mean ± SEM; one experiment). Young (3.5 months) and aged (15 months) WT mice. (a) Fifteen-minute training ($n = 8$ mice per age). Aged mice showed lower performance than did young mice in the 48-hour memory test (age × test effect: $P = 0.0052$, repeated-measures ANOVA; $P = 0.0002$, *t* test). (b) Ten-minute training (different group; $n = 10$ per age). Aged mice did not form 24-hour memory (age × test effect: $P = 0.0021$, repeated-measures ANOVA; $P = 0.01$, *t* test). $^{*}P = 0.01$, $^{**}P = 0.0023$, $^{***}P < 0.0003$ (A, B, and D). See table S3 for detailed statistics.

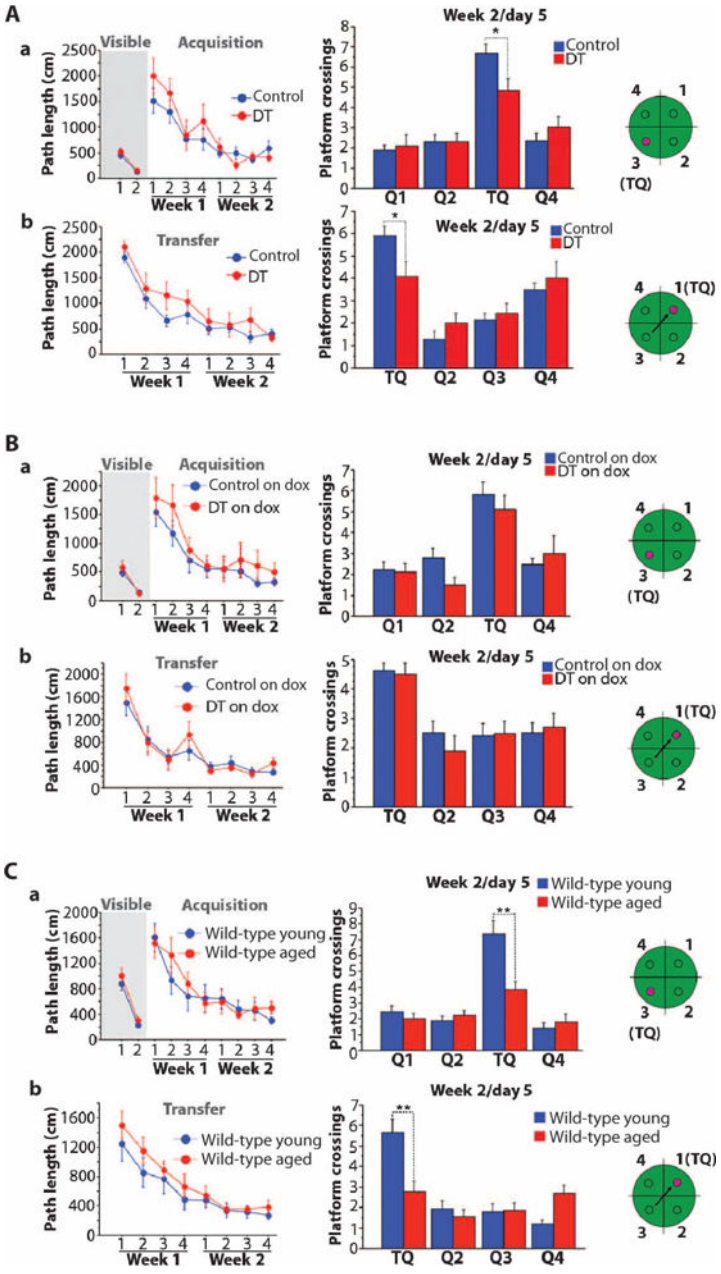

Fig. 4. Effect of RbAp48-DN in the adult forebrain on spatial memory

Mice tested in the Morris water maze. (Left) Path lengths (mean ± SEM) for mice to reach the platform over the days of training. (Right) Number of platform crossings (mean ± SEM) during probe trials 1 day after the end of training. In the probe trial, the platform was removed from the pool and the mice swam for 1 min. The number of times that the mice cross the platform location in the training quadrant (TQ; the quadrant of the pool where the platform was during training) indicates the strength of their spatial memory. (a) Visible and hidden platform versions of the task. (b) Transfer phase of the task (the mice are trained to learn a new hidden platform location). The green schematics depict the quadrants of the pool, and the small circle in them depicts the platform locations. (**A**) DT and control mice

kept off doxycycline in adulthood [same mice as in Fig. 3A (a); DT: $n = 11$ and control: $n = 22$ (tetO = 6, tTA = 8, WT = 8); one experiment]. No differences were observed between DT and controls [$P > 0.137$, repeated-measures ANOVA for visible (a), hidden/acquisition (a), and hidden/transfer (b)]. In the probe trials (right), DT displayed significantly lower performance than did controls [repeated-measures ANOVA, quadrant × genotype effect: $P = 0.04$ (a) and $P = 0.03$ (b); *t* test in training quadrant: $P = 0.017$ (a) and $P = 0.035$ (b)]. (**B**) DT and control groups treated with doxycycline in adulthood [same mice as in Fig. 3B (a); DT on dox: $n = 10$ and control: $n = 17$ (tetO = 5, tTA = 5, WT = 7); one experiment]. No differences were observed (repeated-measures ANOVA; visible/hidden-acquisition/hidden-transfer: $P > 0.16$; probe trials: $P > 0.34$). (**C**) Young adult (3.5 months) and aged (15 months) WT mice ($n = 14$ per age; one experiment). Groups showed similar path lengths during training [$P > 0.1$, repeated-measures ANOVA for (a) and (b)]. During the probe trials, aged mice crossed the platform location significantly less often than did young animals [repeated-measures ANOVA, age × quadrant effect: $P = 0.0003$ (a) and $P = 0.0002$ (b); *t* test for training quadrant: $P = 0.0015$ (a) and $P = 0.002$ (b)]. $*P < 0.036$; $**P < 0.0021$. See table S3 for detailed analysis.

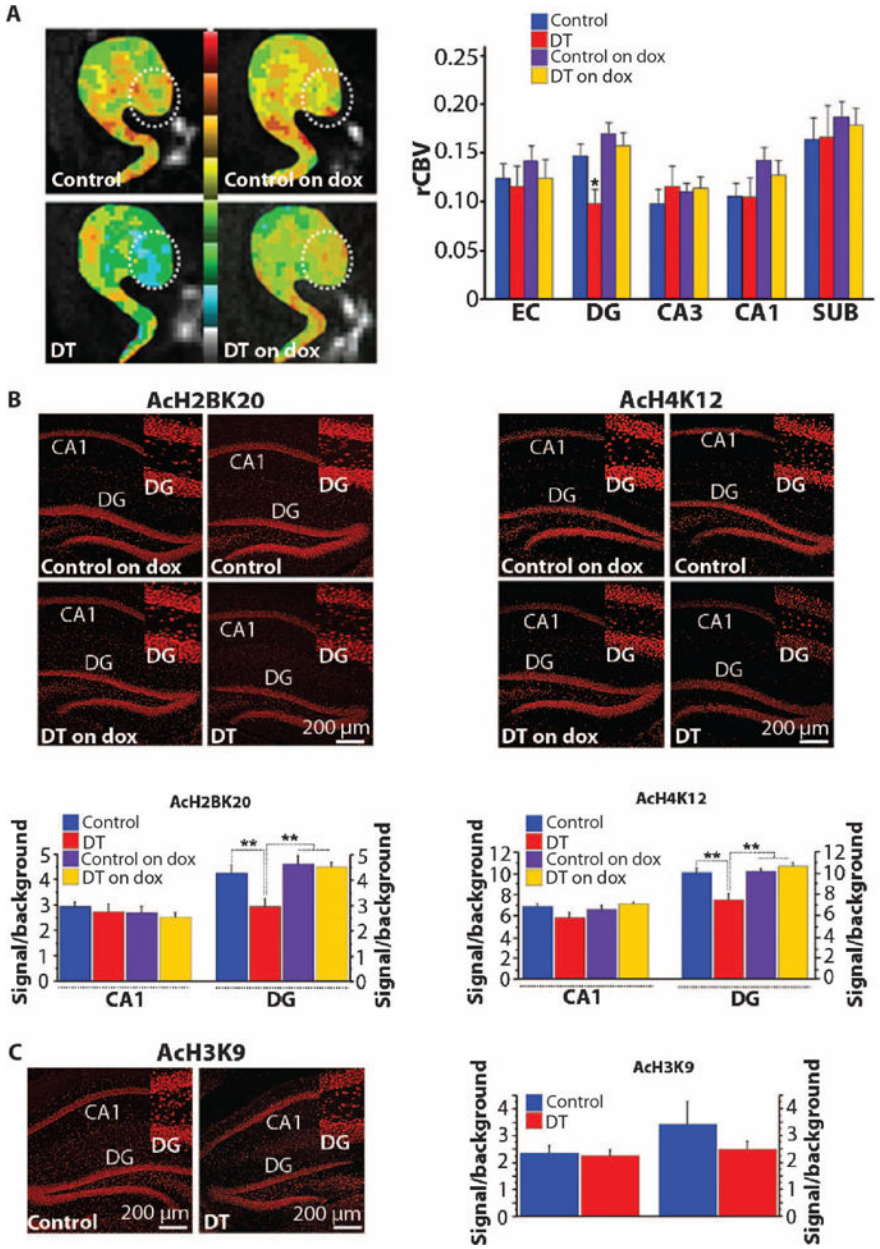

Fig. 5. RbAp48-DN in the DG

(**A**) (Left) Individual examples of CBV maps of the hippocampal formation [EC, DG (circle), CA3-CA1, and subiculum (SUB)], generated with MRI, in DT mice on or off dox in adulthood and respective control siblings. The CBV maps are color-coded such that cooler colors reflect less basal metabolism. (Right) Group data analysis (mean ± SEM) of relative CBV (rCBV) (DT off dox: $n = 9$, controls off dox: $n = 19$, DT on dox: $n = 12$, controls on dox: $n = 15$; one measure per subregion per mouse). Selective decrease in rCBV of DG in DT off dox ($F = 6.3$, $P = 0.019$). (**B**) Immunohistochemistry (top) and quantification (mean ± SEM) (bottom) of AcH2B(Lys^{20}) and AcH4(Lys^{12}). Their levels were significantly reduced in the DG of DT off dox (comparisons with controls off dox and controls and DT on dox; $P < 0.003$, ANOVA). AcH2B(Lys^{20}): DT off dox: $n = 27$ slices (five mice), DT on dox:

n = 15 slices (three mice), controls off dox: n = 45 slices (seven mice), controls on dox: n = 15 slices (four mice). AcH4(Lys^{12}): DT off dox: n = 44 slices (five mice), DT on dox: n = 15 slices (three mice), controls off dox: n = 52 slices (seven mice), controls on dox: n = 11 slices (four mice). (**C**) Immunohistochemistry (left) and quantification (mean ± SEM) (right) of AcH3(Lys^{9}). No differences were observed (P > 0.42, ANOVA). DT off dox: n = 16 slices (five mice), controls off dox: n = 28 slices (seven mice). Mice on dox were not analyzed because no difference was detected in mice off dox. (Insets) High-magnification DG images. (B and C) See tables S1 and S3 for detailed analysis. *P < 0.05; **P < 0.01.

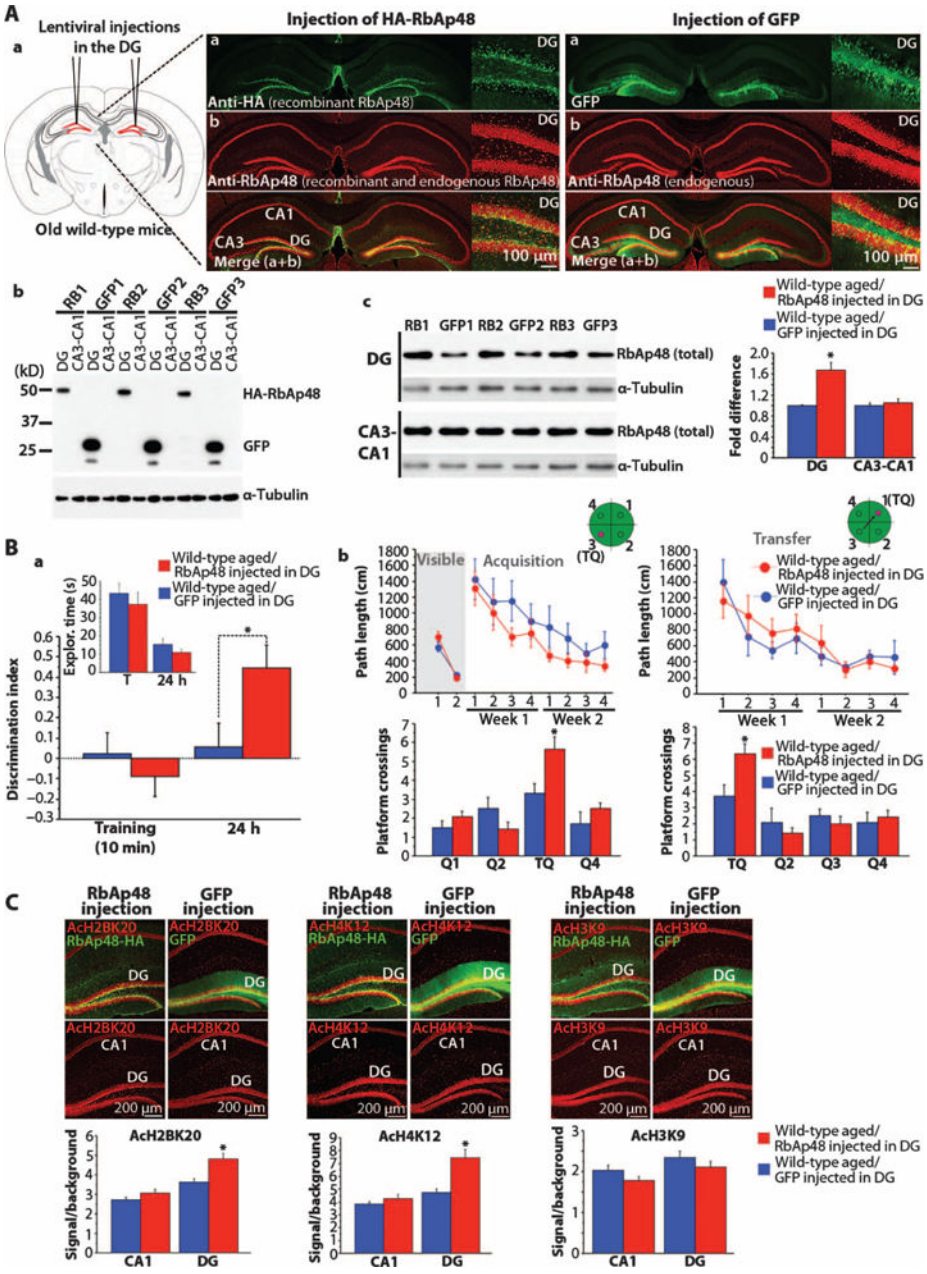

Fig. 6. Effect of RbAp48 up-regulation in the DG on histone acetylation and age-related memory loss

(**A**) (a) Schematic representation and confocal images of the hippocampi from WT aged mice (15 months) expressing DG RbAp48-HA (hemagglutinin) or green fluorescent protein (GFP) (control) via lentiviral injections. (Insets) High-magnification DG images. (b) Western blot showing DG-specific expression of RbAp48-HA and GFP. RB1 to RB3 and GFP1 to GFP3 indicate the numbers of RbAp48-HA– and GFP-injected mice. (c) Western blot and averaged data (±SEM) of total RbAp48. $n = 9$ measures per virus (three mice per virus; three independent blots). Significant increase of RbAp48 in the DG of RbAp48-HA mice compared to GFP controls ($F_{1,16} = 22.584$; $^*P = 0.0002$, ANOVA). RbAp48 level in CA3-CA1 was similar between the two groups ($F_{1,16} = 0.397$; $P = 0.7357$, ANOVA). (**B**)

Data from novel object recognition (a) and the Morris water maze (b) (mean ± SEM; one experiment for each task). (a) RbAp48-HA–injected aged mice (15 months; $n = 12$) performed better than GFP-injected age-matched littermates ($n = 10$) during the 24-hour memory test (injection × session effect: $P = 0.0192$, repeated-measures ANOVA; $P = 0.0275$, t test). (b) (Top) Both groups performed similarly during training in all phases of the water maze (repeated-measures ANOVA; visible: $P = 0.36$; acquisition: $P = 0.0703$; transfer: $P = 0.6996$). (Bottom) RbAp48-HA mice performed better than GFP controls during probe trials 1 day after at the end of training (repeated-measures ANOVA; injection × quadrant effect; acquisition: $P = 0.0094$, t test for training quadrant: $P = 0.0133$; transfer: $P = 0.0443$, t test for training quadrant: $P = 0.016$). *$P < 0.03$. (**C**) Immunohistochemistry and quantification (mean ± SEM) of acetylated histones. AcH2BK20 and AcH4K12 levels were significantly increased in the DG of RbAp48-HA–injected aged mice compared to GFP-injected siblings (*$P < 0.0015$, ANOVA). AcH3K9 remained unaltered in DG and CA3-CA1 ($P > 0.095$, ANOVA). $n = 12$ slices per virus (three mice per virus; four slices per mouse). See tables S1 and S3 for detailed analysis.

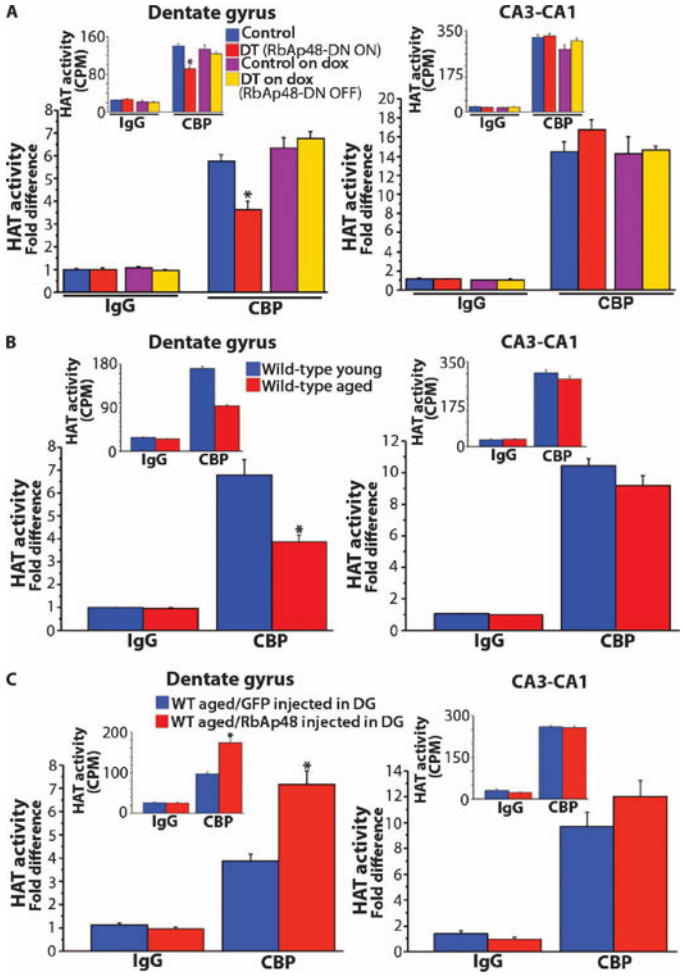

Fig. 7. Effect of expression of RbAp48-DN in the forebrain on CBP HAT activity

Averaged HAT activity (±SEM) of CBP immunoprecipitated from DG and CA3-CA1 lysates expressed as fold difference from IgG control immunoprecipitations. (Insets) Raw data acquired from HAT assays [^{3}H counts per minute (CPM)]. (**A**) Assays in DT mice (3.5 months) and control littermates kept off doxycycline or doxycycline in adulthood. DT, DT off dox; Control, control off dox. $n = 9$ measurements per genotype per treatment (three measurements per immunoprecipitation per mouse; three mice per genotype per treatment). Significantly reduced CBP HAT activity in the DG of DT compared to all other groups ($P < 0.0005$, ANOVA). (**B**) Young (3.5 months) and aged (15 months) WT mice. $n = 12$ measurements per age (three measurements per immunoprecipitation per mouse; four mice per age). Significantly reduced CBP HAT activity in the DG of aged mice ($P = 0.0006$, ANOVA). (**C**) WT aged mice (15 months) virally expressing in DG RbAp48-HA (RbAp48 up-regulation in DG) or GFP (control). $n = 9$ measurements per virus (three measurements per immunoprecipitation per mouse; three mice per virus). CBP HAT activity was significantly increased in the DG of RbAp48-HA mice compared to GFP controls ($P = 0.0001$, ANOVA). *$P < 0.0006$. For detailed analysis, see table S3.

Table 1
Transcripts that decrease or increase with age in the DG in humans

Summarized data from microarray analysis.

Name	GenBank accession no.	Correlation coefficient	*P*
Negative correlations			
RbAp48	X71810.1	−0.94	0.0005
Proteasome subunit β type 7	NM_002799	−0.92	0.001
Mature T cell proliferation 1	Z24459	−0.89	0.003
Pleiotrophin	BC005916	−0.88	0.004
Cullin 5	BF435809	−0.88	0.004
Cadherin 11	D21254	−0.88	0.004
Hypothetical protein SBBI67	NM_020393.1	−0.87	0.005
Chaperonin-containing TCP1	NM_006431	−0.87	0.005
Nucleoside-diphosphate kinase	NM_003551	−0.87	0.005
Positive correlations			
RECQL (DNA helicase)	AI685944	0.93	0.0007
DnaJ homolog, subfamily C, member 4	AW024467	0.93	0.0009
RAB11B (RAS oncogene family)	AL575337	0.92	0.001
Dematin	NM_001978	0.92	0.001
Topoisomerase-related function protein 4	NM_006999	0.89	0.003
ClpX caseinolytic protease X homolog	NM_006660	0.87	0.005
Oxidized low-density lipoprotein receptor 1	AF035776.1	0.87	0.005
Box polypeptide 21	NM_004728.1	0.87	0.005